(J. Stat. Mech. P02057, 2009)

Stochastic approach and fluctuation theorem for ion transport

David Andrieux and Pierre Gaspard
Center for Nonlinear Phenomena and Complex Systems,
Université Libre de Bruxelles, Code Postal 231, Campus Plaine, B-1050 Brussels, Belgium

We present a stochastic approach for ion transport at the mesoscopic level. The description takes into account the self-consistent electric field generated by the fixed and mobile charges as well as the discrete nature of these latter. As an application we study the noise in the ion transport process, including the effect of the displacement current generated by the fluctuating electric field. The fluctuation theorem is shown to hold for the electric current with and without the displacement current.

I. INTRODUCTION

The study of electrolyte solutions finds its origin in the seminal works of Nernst [1, 2] and Planck [3, 4]. Ion transport in electrolytes is described as arising from a diffusive part due to the concentration gradients and a drift part due to the external electric field imposed to the system. A more accurate description is obtained if the electrical field is not only generated by external means but also self-consistently incorporates the contributions of the local deviations from electroneutrality [5, 6]. Under the assumption that the electric field propagates instantaneously - the quasi-static limit of the Maxwell equations - this problem is known as the Nernst-Planck-Poisson (NPP) problem [7, 8]. Here, the electric field self-consistently arises from the distribution of charges as described by the Poisson equation. In this case, the transport process may present an additional contribution due to the temporal variations of the electric field, known as the displacement current [9–11]. This approach has also played a basic role in the theory of other systems: Indeed, the NPP equations, combined with statistical arguments, lead for instance to the description of semiconductor p-n junctions [12, 13].

On the other hand, ionic solutions exist in many natural or artificial systems. Many biological processes crucially depend on the transport of ions, e.g., between intra- and extracellular solutions [14, 15]. Besides, solid-state nanopores are fabricated for the study of ionic current fluctuations [16]. In these systems, the transport of ion takes place in different geometries, either with the complexity of channel proteins or more regular as straight channels in the case of nanopores. Biological ion channels [17], as well as physico-chemical systems such as nanopores [18], nanofluidic diodes [19], or nanostructures studied by impedance spectroscopy [20], are often described by the NPP theory. Yet, they are of mesoscopic sizes and, at these scales, the motion of ions in solution is subjected to molecular fluctuations and presents a stochastic behavior. These random fluctuations can be successfully described at the mesoscopic level as Markovian stochastic processes [21–25]. Non-Markovian discrete-state models have also been considered to take into account the memory effects resulting, in particular, from the lumping of diffusion [26]. The description to be adopted depends on the geometry. In short heterogeneous channels, transport tends to proceed by jumps between discrete states corresponding to wells in the free-energy potential. In long homogeneous channels such as cylindrical nanopores, diffusion is not interrupted by barriers except at entrance and exit. In any case, the master equation ruling these stochastic processes should reduce to the evolution equation for the charges densities at the macroscopic level. In this respect, one of the fundamental problems is to incorporate the long-range Coulomb interaction between the electric charges in the description.

In the present work, our purpose is to present a description of ion transport which is consistent with the laws of both electricity and statistical thermodynamics. The key point is that the long-range Coulomb interaction deeply influences the fluctuations of the particle and total currents. The proposed model describes the spatial distribution of the discrete number of ions in a long channel. The ions undergo random jumps due to the thermal agitation in a self-consistently generated electrical potential landscape. This description takes into account the stochastic aspects of the time evolution as well as the self-consistent electric field generated by the charge distribution. In this regard, it offers a computationally favorable alternative to more expensive techniques such as Brownian dynamics [27, 28]. This approach allows us to study various aspects of ion transport, revealing, e.g., the long-ranged spatial correlations of the potential fluctuations inside the channel. We further study the fluctuations present in the transport process, including the contributions of the displacement current. Also, we show that the fluctuation theorem [29–36] describing the large-deviation properties of the current holds in this case as well.

The paper is organized as follows. In Sec. II, we introduce the macroscopic description of ion transport in terms

of the Nernst-Planck-Poisson equations. The stochastic description is presented in Sec. III. The fluctuations in the ion transport process are studied in Sec. IV. In Sec. V, the symmetry of the fluctuation theorem is shown to hold for both the particle and electric currents. Conclusions are drawn in Sec. VI.

II. MACROSCOPIC EQUATIONS

We consider a one-dimensional conduction channel extending from $x = 0$ to $x = \ell$. An important class of electrolytic systems are those which contain a homogeneous distribution of immobile ions [37]. We therefore consider a model with a single mobile species of charge e and density n being transported in a channel presenting a fixed ion density n_- of opposite charge $-e$. The charge density inside the system is thus given by

$$\rho = e(n - n_-)\,. \tag{1}$$

The case of several fixed and mobile species can be treated in a similar way. Expressing the electric field $\boldsymbol{\mathcal{E}}$ in terms of the electric potential Φ as $\boldsymbol{\mathcal{E}} = -\boldsymbol{\nabla}\Phi$, the problem is ruled by the coupled diffusion and Poisson equations:

$$\partial_t n \;=\; \boldsymbol{\nabla}\cdot(D\boldsymbol{\nabla}n + \mu e n \boldsymbol{\nabla}\Phi)\;, \tag{2a}$$

$$\nabla^2\Phi \;=\; -\frac{e}{\epsilon}(n - n_-)\,. \tag{2b}$$

D is the diffusion coefficient of the mobile species and μ is the mobility coefficient which is given by Einstein's relation $\mu = D/k_{\rm B}T$. The dielectric fluid is here homogeneous throughout the channel and has a dielectric constant of ϵ. Equation (2a) is the conservation equation for the particle density, $\partial_t n = -\boldsymbol{\nabla}\cdot\boldsymbol{J}$, where $\boldsymbol{J}$ is the particle current density. The Poisson equation (2b) in turn gives the electric potential as a function of the charge density. This coupled system (2) forms the Nernst-Planck-Poisson equations. They correspond to the quasi-static limit of the complete Maxwell equations. On the other hand, the total current density reads [9, 11]

$$\boldsymbol{I} = e\boldsymbol{J} + \epsilon\frac{\partial\boldsymbol{\mathcal{E}}}{\partial t}\,, \tag{3}$$

the last term being the displacement current density arising from temporal variations of the electrical field. The displacement current vanishes in a stationary state but contributes, for example, when the system relaxes toward the stationary state. Note that, by virtue of the Poisson equation (2b), the total current density is divergence free, $\boldsymbol{\nabla}\cdot\boldsymbol{I} = 0$, *at all times*. We further notice that the experimentally measurable quantity is given by the total current [11].

The channel is in contact with two reservoirs of particles maintained at fixed concentrations and electric potentials. Equations (2) are thus supplemented by the boundary conditions

$$n(0) \;=\; n_{\rm L}\,, \quad n(\ell) = n_{\rm R}\,, \tag{4a}$$

$$\Phi(0) \;=\; \Phi_{\rm L}\,, \quad \Phi(\ell) = \Phi_{\rm R}\,, \tag{4b}$$

determining the concentrations on the left (L, $x = 0$) and right (R, $x = \ell$) boundaries as well as the external potential difference $V = \Phi_{\rm L} - \Phi_{\rm R}$ applied to the channel.

For time-independent boundary conditions, the system evolves toward a stationary state where $\partial_t n = 0$ so that the particle current density $\boldsymbol{J}$ is constant in time and in space. For the one-dimensional channel here considered, the stationary density satisfying the boundary conditions (4) is expressed as

$$n(x) = n_{\rm L}{\rm e}^{\phi(x)-\phi_{\rm L}} - \frac{J}{D}\,{\rm e}^{\phi(x)}\int_0^x {\rm e}^{-\phi(y)}\,dy\,, \tag{5}$$

along with the particle current

$$J = -D\,\frac{n_{\rm R}{\rm e}^{-\phi_{\rm R}} - n_{\rm L}{\rm e}^{-\phi_{\rm L}}}{\int_0^\ell {\rm e}^{-\phi(x)}dx}\,, \tag{6}$$

where we introduced the dimensionless potential $\phi \equiv -e\Phi/k_{\rm B}T$ to simplify the expressions. This potential obeys the dimensionless Poisson equation

$$\nabla^2\phi = \frac{1}{\lambda^2}\left(\frac{n}{n_-} - 1\right)\,, \tag{7}$$

where

$$\lambda \equiv \sqrt{\frac{\epsilon k_{\rm B} T}{e^2 n_-}} \tag{8}$$

is the Debye screening length of the system [38].

The stationary state is a state of thermodynamic equilibrium if the particle current vanishes, i.e., when we have

$$(\phi_{\rm L} - \phi_{\rm R})_{\rm eq} = \ln \frac{n_{\rm L}}{n_{\rm R}} \qquad \text{or} \qquad (\Phi_{\rm L} - \Phi_{\rm R})_{\rm eq} = \frac{k_{\rm B} T}{e} \ln \frac{n_{\rm R}}{n_{\rm L}} \,. \tag{9}$$

This voltage difference is known as the Nernst potential [1, 2]. If this condition is not satisfied we are in a nonequilibrium situation characterized by the presence of a non-vanishing ionic current given by Eq. (6). In the stationary state, the associated total current reads

$$I = eJ \tag{10}$$

since the displacement current vanishes in this case. However, at the mesoscopic level, fluctuations in the charge distribution generate a fluctuating displacement current, as studied in Sec. IV.

III. STOCHASTIC DESCRIPTION

The study of noise and molecular fluctuations at the mesoscopic scale is successfully accomplished in terms of a Markovian random processes. Indeed, the master equation is known to describe the fluctuations down to the mesoscopic scale [21–23].

We here introduce a stochastic model for the distribution of ions in the channel that incorporates the self-consistent electric field generated by the fluctuating distribution of ions. The channel is divided into L cells of volume ΔV, cross section σ, and length $\Delta x = \ell/L$ centered at the positions $x_i = (i - 1/2)/\Delta x$ $(i = 1, \ldots, L)$. Each cell contains a discrete number of mobile ions N_i and a constant number $N_- = n_- \Delta V$ of fixed ions. The cells 0 and $L+1$ correspond to the external reservoirs maintained at fixed concentrations so that their particle numbers N_0 and N_{L+1} remain constant in time. The dimensionless electric potential $\phi_i = -e\Phi_i/k_{\rm B}T$ is defined on each cell as well. It obeys the Poisson equation (7) which is discretized according to

$$\frac{\phi_{i+1} - 2\phi_i + \phi_{i-1}}{\Delta x^2} = \frac{1}{\lambda^2} \left(\frac{N_i}{N_-} - 1 \right) \tag{11}$$

with the boundary conditions $\phi_0 = \phi_{\rm L}$ and $\phi_{L+1} = \phi_{\rm R}$. Equations (11) form a linear system that must be solved at each time the particle distribution changes. Its exact solution is given in Appendix A. The extension of the model to several (positive or negative) ion species and inhomogeneous distribution of fixed ions and permittivity is straightforward.

The state of the system is determined by the number of ions N_i in each cell. The evolution equation for the probability distribution $P(N_1, ..., N_L)$ to observe a configuration $\{N_i\}$ of particles is ruled by the master equation

$$\begin{aligned} \frac{d}{dt} P(N_1, ..., N_L) = \sum_{i=0}^{L} \; \Big[& \; W_{+i}(..., N_i + 1, N_{i+1} - 1, ...) P(..., N_i + 1, N_{i+1} - 1, ...) \\ & - \; W_{+i}(..., N_i, N_{i+1}, ...) P(..., N_i, N_{i+1}, ...) \\ & + \; W_{-i}(..., N_i - 1, N_{i+1} + 1, ...) P(..., N_i - 1, N_{i+1} + 1, ...) \\ & - \; W_{-i}(..., N_i, N_{i+1}, ...) P(..., N_i, N_{i+1}, ...) \; \Big] \end{aligned} \tag{12}$$

where $W_{\pm i}(\cdot)$ denotes the transition rate between two configurations of the system. The transition $\pm i$ changes the configuration from $(..., N_i, N_{i+1}, ...)$ to $(..., N_i \mp 1, N_{i+1} \pm 1, ...)$. These transitions rates are supplemented with the boundary conditions that N_0 and N_{L+1} take fixed values.

The transition rates can be expressed as

$$W_{+i}(..., N_i, N_{i+1}, ...) \; = \; \psi(\Delta U_{i,i+1}) N_i \tag{13}$$

$$W_{-i}(..., N_i, N_{i+1}, ...) \; = \; \psi(\Delta U_{i+1,i}) N_{i+1} \tag{14}$$

with the function

$$\psi(\Delta U) = \frac{D}{\Delta x^2}\frac{\beta\Delta U}{\mathrm{e}^{\beta\Delta U}-1} \tag{15}$$

where D is the diffusion coefficient and $\beta = (k_{\mathrm{B}}T)^{-1}$ the inverse temperature. The prefactor $D/\Delta x^2$ allows us to recover the appropriate evolution equation (2a) in the macroscopic limit, $L \to \infty$ [39]. The transition rates are proportional to the number of mobile ions in the cells and depend on the free electrostatic energy difference $\Delta U_{i,i+1}$ as a result of the transition event:

$$\Delta U_{i,i+1} = \frac{e}{2}(V_i + V_i')\,. \tag{16}$$

In Eq. (16), V_i and V_i' are the voltage drops across the cells i and $i+1$ before and after a transition event, respectively. This expression corresponds to the change in electrostatic energy resulting from the transition event, as shown in Appendix A. Consequently, Eq. (16) can be expressed as

$$\Delta U_{i,i+1} = \frac{e}{2}(\Phi_{i+1} - \Phi_i + \Phi_{i+1}' - \Phi_i') \tag{17}$$

in terms of the electric potential calculated for the current configuration, $\Phi_j = \Phi_j(N_1, ..., N_L)$, and the electric potential Φ_j' that would occur if the corresponding transition $\pm i$ were performed:

$$\Phi_j' = \Phi_j'(..., N_i \mp 1, N_{i+1} \pm 1, ...)\,. \tag{18}$$

The potential Φ_j' can be expressed as

$$\Phi_j' = \Phi_j \mp e\left(\mathsf{C}^{-1}\right)_{j,i} \pm e\left(\mathsf{C}^{-1}\right)_{j,i+1} \tag{19}$$

in terms of the matrix C^{-1} obtained from the solution of the discretized Poisson equation (see Appendix A).

The function ψ satisfies the identity

$$\psi(\Delta U) = \psi(-\Delta U)\mathrm{e}^{-\beta\Delta U} \tag{20}$$

which guarantees that detailed balance is fulfilled at equilibrium [40–42]. On the other hand, the nonequilibrium constraints or affinities driving the system out of equilibrium [43] can be identified in the stochastic description thanks to a construction put forward by Schnakenberg [22], according to which the affinities are obtained from the cyclic trajectories in the forward and backward directions. In our case, as verified in Appendix B, the macroscopic affinity is readily identified by considering trajectories involving the transfer of an ion from one reservoir to the other, yielding

$$A = \ln\left(\frac{N_0}{N_{L+1}}\mathrm{e}^{\Delta\phi}\right) = \ln\left(\frac{n_{\mathrm{L}}}{n_{\mathrm{R}}}\mathrm{e}^{\Delta\phi}\right)\,. \tag{21}$$

Here, $\Delta\phi = \phi_{\mathrm{R}} - \phi_{\mathrm{L}}$ and we note that this affinity only involves macroscopic quantities as it should. At equilibrium the affinity vanishes, $A_{\mathrm{eq}} = 0$, and we recover the macroscopic equilibrium condition (9).

The stochastic process is simulated as follows. Random trajectories of the system are obtained using Gillespie's algorithm [44], which is known to reproduce the statistical properties of the master equation (12). At each random jump, we have to recalculate the electric potential in the channel by solving the system (11). The simulations are performed with the following parameters. Each cell contains a number $N_- = 25$ of fixed ions. By an appropriate choice of the time unit, we can impose for example $D/\Delta x^2 = 1$. Using the dimensionless electric potential ϕ, the only remaining dimensional parameter is the Debye length λ. We form the dimensionless quantity ℓ/λ, i.e., the ratio between the channel and Debye's length, for which we choose the value $\ell/\lambda = 50$. For a Debye length of 7 nm this would correspond to a channel length of 350 nm.

The link with the macroscopic description is established in the limit where the volume of the cells ΔV vanishes in which case the concentrations are recovered as $n(x_i) = \langle N_i\rangle/\Delta V$. In Fig. 1a, we depict the average number of ions along the channel, estimated by the time average

$$\langle N_i\rangle = \lim_{T\to\infty}\frac{1}{T}\int_0^T N_i(t)dt \tag{22}$$

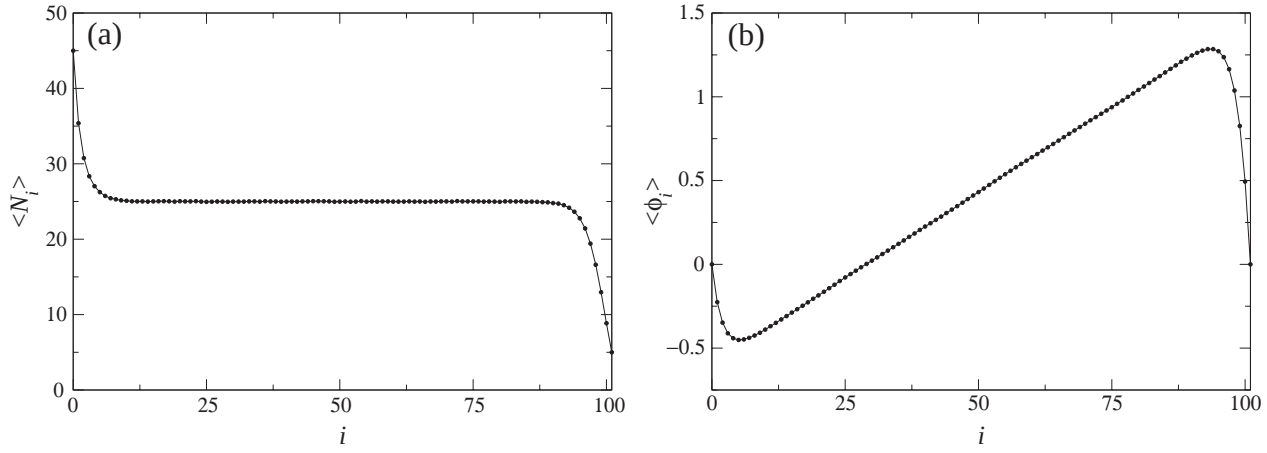

FIG. 1: (a) Mean number of ions $\langle N_i \rangle$ as a function of the position i in the channel. (b) Mean dimensionless electric potential $\langle \phi_i \rangle$ as a function of the position i in the channel. The channel is composed of $L = 100$ cells, each with $N_- = 25$ fixed ions. The channel is submitted to the boundary conditions $N_{\rm L} = 45$, $N_{\rm R} = 5$, and $\phi_{\rm L} = \phi_{\rm R}$.

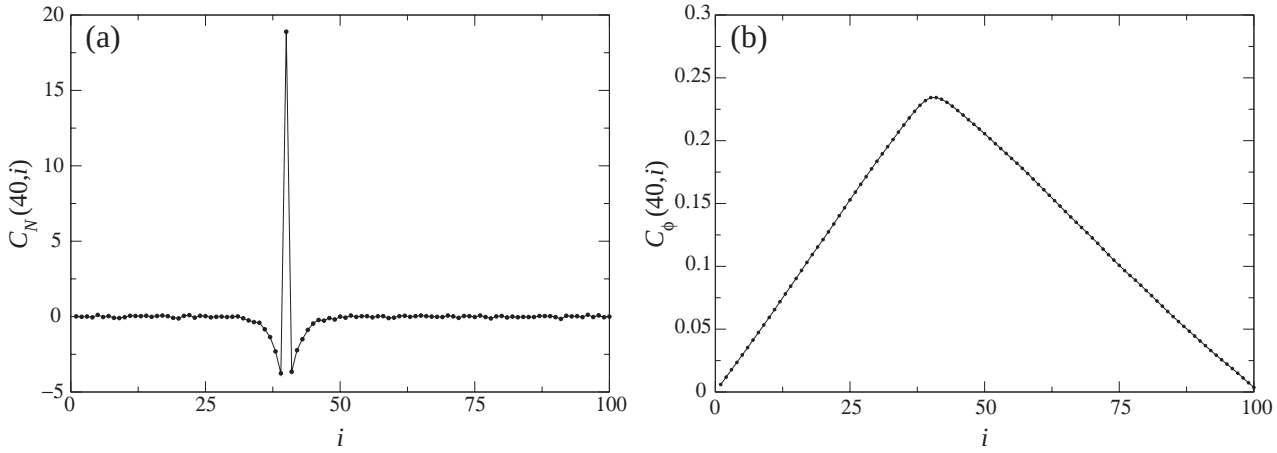

FIG. 2: (a) Spatial correlations $C_N(40, i)$ for the density fluctuations between site 40 and site i as a function of the position i in the channel. (b) Spatial correlations $C_\phi(40, i)$ for the electric potential fluctuations between site 40 and site i as a function of the position i in the channel. The channel is composed of $L = 100$ cells, each containing $N_- = 25$ fixed ions. The boundary conditions are $N_{\rm L} = 45$, $N_{\rm R} = 5$, and $\phi_{\rm L} = \phi_{\rm R}$.

which, by ergodicity, is equivalent to the ensemble average $\langle N_i \rangle = \sum N_i P(..., N_i, ...)$. We see that electroneutrality, $\langle N_i \rangle \simeq N_-$, is well respected except for a small layer from the boundaries over a distance of the order of the screening distance λ. The corresponding mean electric potential $\langle \phi_i \rangle$ is shown in Fig. 1b. It is approximately linear throughout the channel, which corresponds to a constant electric field, except again for a small layer near the boundaries.

Due to the electric interaction, the particle density fluctuations present spatial correlations along the channel. The correlations between cells are obtained by the time averages

$$C_N(i,j) \equiv \langle N_i N_j \rangle - \langle N_i \rangle \langle N_j \rangle = \lim_{T\to\infty} \frac{1}{T} \int_0^T [N_i(t) - \langle N_i \rangle] [N_j(t) - \langle N_j \rangle] \, dt \,. \tag{23}$$

Fig. 2a shows the effect of the electric interaction on the spatial correlations. We observe negative correlations between neighboring sites, showing that an excess charge at some location induces a repulsive effect on the neighboring sites. The negative correlations rapidly diminish with the separation between sites over a distance comparable to the Debye length. The presence of such correlations also shows that the particle distribution is not Poissonian even at equilibrium in contrast with population dynamics of chemical reactions network [23]. The electric potential correlation function

$$C_\phi(i,j) \equiv \langle \phi_i \phi_j \rangle - \langle \phi_i \rangle \langle \phi_j \rangle \tag{24}$$

is depicted in Fig. 2b. It presents long-range correlations with a linear decrease in both directions between the site and the boundaries.

IV. FLUCTUATIONS IN ION TRANSPORT

In this section, we study the fluctuations in the transport process. For this purpose, we first introduce the fluctuating particle current j_k counting the number of ions transferred between the cells k and $k+1$. We denote by $\varepsilon_k(s) = \pm 1$ the discrete charge transfer of an ion in the positive or negative direction between the cells k and $k+1$ during the s^{th} random transition occurring at the time t_s [$\varepsilon_k(s) = 0$ otherwise]. Accordingly, the fluctuating particle current is given by

$$j_k(t) = \sum_{s=-\infty}^{+\infty} \varepsilon_k(s)\delta(t - t_s)\,. \tag{25}$$

We notice that the currents (25) are so-called point processes composed of singular events occurring at random times. In the stationary state, the average particle current crossing the channel is time-independent and can be obtained from the stationary probability distribution as

$$J \equiv \langle j_k(t)\rangle = \sum_{N_1,\ldots,N_L} P_{\text{st}}(N_1,...,N_L)[W_{+k}(N_1,...,N_L) - W_{-k}(N_1,...,N_L)]\,. \tag{26}$$

By current conservation, the average particle current is independent of the position in the channel, $J \equiv \langle j_k\rangle$ for all k.

However, the experimentally measured electric current is composed of the particle and displacement currents according to Eq. (3). Indeed, even in a stationary state, fluctuations in the particle distribution at the mesoscopic level generate a fluctuating electric field that, in turn, generates a fluctuating contribution to the electric current. We thus calculate the change in the electric field associated with the random jumps of the charge carriers. The change in the electric field between the cells k and $k+1$, $E_{k+1/2} = -(\Phi_{k+1} - \Phi_k)/\Delta x$, is expressed as

$$-\frac{1}{\Delta x}\Big(\Phi'_{k+1} - \Phi'_k - \Phi_{k+1} + \Phi_k\Big) = \pm\frac{e}{\Delta x}\Big[\Big(\mathsf{C}^{-1}\Big)_{k+1,l} - \Big(\mathsf{C}^{-1}\Big)_{k+1,l+1} - \Big(\mathsf{C}^{-1}\Big)_{k,l} + \Big(\mathsf{C}^{-1}\Big)_{k,l+1}\Big] \tag{27}$$

if the transition $W_{\pm l}$ is performed. The second equality is obtained by using Eq. (19) for the potential $\Phi'(...,N_l \mp 1, N_{l+1} \pm 1, ...)$ after the transition. The associated displacement current is given by $\epsilon\sigma$ times the change in the electric field, where σ is the cross section of the channel ($\sigma\Delta x = \Delta V$). The displacement current associated with the transition $W_{\pm l}$ and measured between the cells k and $k+1$ thus reads

$$\begin{cases} \pm e\frac{1}{L+1} & \text{if} \quad k \neq l \\ \mp e\frac{L}{L+1} & \text{if} \quad k = l \end{cases} \tag{28}$$

where we used expression (A7) and the equality $\epsilon\sigma = \alpha\Delta x$. Now, the contribution of the transition $W_{\pm l}$ to the total current is the sum of the particle current, $\pm e$ if $k = l$ and zero otherwise, and the displacement current (28) so that the location l contributes to the total current by the amount

$$\frac{e}{L+1}\, j_l(t) \tag{29}$$

as it should since the electric current must be divergence free at all times. Remarkably, all the transitions $\pm l$ contribute equally to the electric current. The total current is finally obtained by summing the contributions from all the transitions $\pm l$:

$$I(t) = \frac{e}{L+1}\sum_{l=0}^{L} j_l(t)\,. \tag{30}$$

The sum runs over all the possible charge transfers since each charge displacement in the system modifies the electric field, inducing in turn a displacement current. Expression (30) can also be obtained from the Ramo-Shockley theorem [11, 45–47] linking the current flowing in the external circuit to charge movement inside the system. By virtue of Eq. (26), the mean total current is related to the mean particle current according to

$$\langle I\rangle = eJ\,, \tag{31}$$

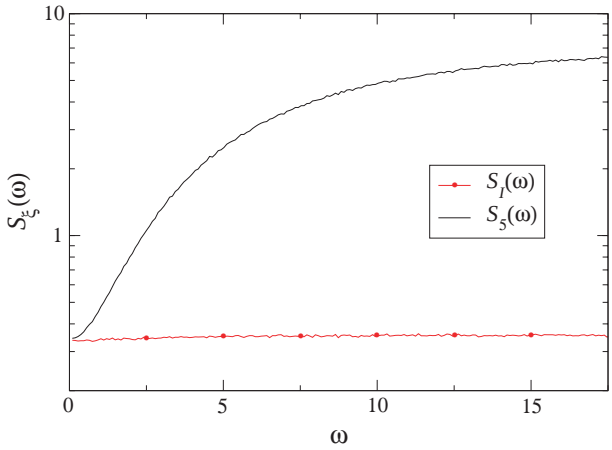

FIG. 3: Power spectra of the particle current (evaluated at $k = 5$) and of the total current in units of e^2 (line with dots). The channel is composed of $L = 20$ cells and is submitted to the boundary conditions $N_{\rm L} = 5$, $N_{\rm R} = 45$, and $\phi_{\rm L} = \phi_{\rm R}$. Each cell contains $N_- = 25$ fixed ions.

showing that the displacement current does not contribute on average, as it should. However, as shown below, the particle and total currents differ in the properties of their non-zero frequency fluctuations.

Besides the mean currents, the noise characterization offers further information on the transport process [11]. The power spectra of the currents are defined as the Fourier transform of the current correlation function:

$$S_\xi(\omega) = \frac{1}{2\pi}\int_{-\infty}^{+\infty} \mathrm{e}^{i\omega t}\Big[\,\langle \xi(t)\xi(0)\rangle - \langle\xi\rangle^2\,\Big]dt\,, \tag{32}$$

where ξ is associated with either the particle current correlations, $\xi = j_k$, or to the electric current, $\xi = I$. These power spectra can be obtained from an ensemble of long random trajectories according to

$$S_\xi(\omega) = \lim_{T\to\infty}\frac{1}{2\pi T}\left\langle |\tilde\xi(\omega)|^2\right\rangle - \langle\xi\rangle^2\,\delta(\omega) \tag{33}$$

where $\tilde\xi(\omega) \equiv \int_0^T \mathrm{e}^{-i\omega t}\xi(t)dt$ and where $\langle\cdot\rangle$ denotes an average over several trajectories. For the particle current, we thus have

$$\tilde j_k(\omega) = \int_0^T \mathrm{e}^{-i\omega t} j_k(t)dt = \sum_s \varepsilon_k(s)\,\mathrm{e}^{-i\omega t_s}\,. \tag{34}$$

Similarly, the power spectrum of the total current (30) is obtained from

$$\tilde I(\omega) = \int_0^T \mathrm{e}^{-i\omega t} I(t)dt = \frac{e}{L+1}\sum_l\sum_s \varepsilon_l(s)\,\mathrm{e}^{-i\omega t_s} \tag{35}$$

where the sums take into account every transition in the system, in accord with Eq. (30).

In Fig. 3, we depict the power spectrum of the particle and total currents. We see that, under the same conditions, they are qualitatively different from each other, showing that the inclusion of the displacement current affects the fluctuations at positive frequencies and therefore must be properly taken into account. The power spectrum of the particle current increases with the frequency ω because the corresponding correlation function is negative. Such anticorrelations constitute another signature of the Coulomb repulsion between the ions, which reduces the probability of a definite transition event after jumping through the same section in the same direction. This frequency dependence of the power spectrum reflects the memory effects induced by the long-range Coulomb interaction on the random motion of the particles. On the other hand, the total current presents a strongly reduced noise at all frequencies because of the long-range correlations induced by the changes in the distribution of charges. We note that the power spectra reach a constant positive value in the high-frequency limit that results from the intrinsic randomness found at all times scales in such stochastic processes [48]. Precisely, in this limit, the spectra S_k are given by the shot-noise formula

$$S_k(\infty) = \sum_{N_1,\ldots,N_L} P_{\rm st}(N_1,\ldots,N_L)[W_{+k}(N_1,\ldots,N_L) + W_{-k}(N_1,\ldots,N_L)]\,. \tag{36}$$

In addition, in the high-frequency limit, the different noise processes become uncorrelated so that

$$S_I(\infty) = \frac{e^2}{(L+1)^2} \sum_{k=0}^{L} S_k(\infty)\,. \tag{37}$$

In the bulk of the channel away from the boundaries by a few Debye's lengths, the spectra $S_k(\omega)$ turn out to be uniform, i.e., approximately independent of the location k. This explains that, for a channel longer than Debye's length, we approximately find

$$S_I(\infty) \simeq \frac{e^2}{L+1} S_k(\infty)\,, \tag{38}$$

as observed in Fig. 3.

Furthermore, when the applied voltage $V = \Phi_L - \Phi_R$ is sufficiently large we may neglect the backward transitions, $W_{-k}(N_1, ..., N_L) \simeq 0$, in which case Eqs. (26) and (36) coincide so that

$$S_k(\infty) = \frac{\langle I \rangle}{e} \tag{39}$$

and

$$S_I(\infty) = \frac{e^2}{L+1} S_k(\infty) = \frac{e\,\langle I \rangle}{L+1} \tag{40}$$

by virtue of Eq. (37). These expressions correspond to the Schottky noise formulae [49].

V. FLUCTUATION THEOREM FOR THE CURRENTS

In this section, we focus on the fluctuations of the particle and total currents in the zero-frequency limit or, equivalently, in the long-time limit. More precisely, we will focus on the full probability distribution of the currents, which contain the information on the second-order noise properties as well as information on higher-order properties. In Ref. [34] it was shown in that the probability distribution of the particle current fluctuations may obey in the long-time limit, $t \to \infty$, a fluctuation symmetry of the form

$$P_k\left[\frac{1}{t}\int_0^t j_k(t')dt' = \alpha\right] \simeq P_k\left[\frac{1}{t}\int_0^t j_k(t')dt' = -\alpha\right] \mathrm{e}^{\alpha A t}\,, \tag{41}$$

where A is the affinity (21). Here, this symmetry holds as a result of the thermodynamic properties of our stochastic description, detailed in Appendix B. An illustration of this relation is given in Fig. 4a where we depict the probability distribution function of the particle current, which is compared to the prediction of the fluctuation theorem (41).

In addition, we here show that the fluctuation theorem also holds for the total current (30) exactly in the same form:

$$P_I\left[\frac{1}{t}\int_0^t I(t')dt' = \alpha\right] \simeq P_I\left[\frac{1}{t}\int_0^t I(t')dt' = -\alpha\right] \mathrm{e}^{\alpha A t}\,. \tag{42}$$

This symmetry can be rigorously shown by extending the demonstration of Ref. [34] to the present situation where any charge displacement in the system induces a non-local contribution to the total current, as shown by Eq. (30). The symmetry relation (42) is illustrated in Fig. 4b. The fluctuation relations (41) and (42) describe the large nonequilibrium current fluctuations and have important consequences on the linear and nonlinear response properties [50].

These results show that the fluctuation theorem is verified for systems of particles interacting with complex, long-ranged interaction, whereas most fluctuation relations were verified for locally interacting particles, for example with purely diffusive [51] or effusive [52] behavior, or with hard-core interaction [53]. For ion transport in channels, the fluctuation theorem was considered in the limiting case where the electric repulsion is strong enough to prevent the presence of more than one ion inside the channel [51, 54–56].

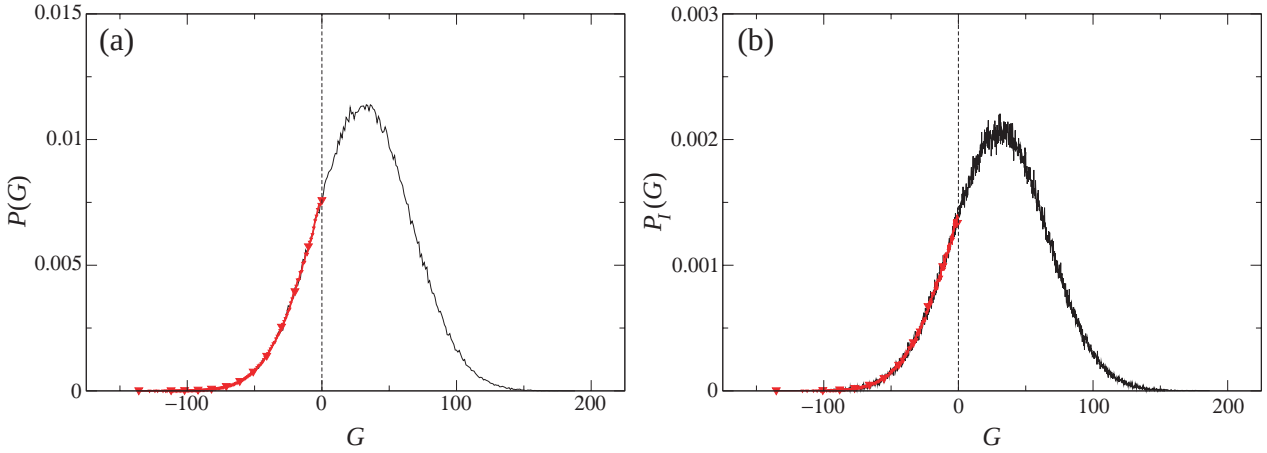

FIG. 4: (a) Probability distribution of the integrated particle current, $G = \int_0^t j_k(t')dt'$, evaluated at $k = 2$. The comparison is performed with the fluctuation symmetry (41) for the negative part of the distribution (thick line with triangles). (b) Probability distribution of the integrated electric current, $G = (1/e)\int_0^t I(t')dt'$. The comparison is performed with the fluctuation symmetry (42) for the negative part of the distribution (thick line with triangles). The channel is composed of $L = 10$ cells, each containing $N_- = 25$ fixed ions. The probability distributions are evaluated at time $t = 273$. The channel is submitted to the boundary conditions $N_{\rm L} = N_{\rm R} = 25$ and $\phi_{\rm R} - \phi_{\rm L} = 0.05$ so that the affinity takes the value $A = 1/20$.

VI. CONCLUSIONS

In this paper, we have introduced a mesoscopic description of ion transport in homogeneous channels on the ground of the laws of both electricity and statistical thermodynamics. The model is ruled by a master equation describing the spatial distribution of the discrete numbers of ions in the channel. Indeed, the stochastic aspects of the time evolution as well as the discrete nature of the ions are essential aspects of the behavior of matter at the mesoscopic scale. The model incorporates the self-consistent field generated by the fixed and mobile ions as described by the Poisson equation. Also, the model is shown to be consistent with thermodynamics and can be studied under equilibrium or nonequilibrium conditions.

The stochastic description can be used to obtain the spatial correlations of particle density fluctuations in the channel, which reveal the strong repulsion due to the electric interaction for fluctuations that depart from electroneutrality. Moreover, we observe long-range correlations in the electric potential fluctuations.

Another quantity of fundamental interest in the study of ion transport in channels is the experimentally measured total current, which is composed of the particle current plus the displacement current arising from the temporal variations of the electric field. At the macroscopic level, the displacement current vanishes in a stationary state. On the other hand, at the mesoscopic level, the molecular fluctuations induce long-ranged electric field fluctuations which result in a reduced noise spectrum at all positive frequencies. The particle and total currents thus differ in their fluctuation properties and the present approach allows us to assess the importance of such effects. Furthermore, we have shown that the fluctuation theorem for the currents holds in this more general situation as well, that is when the displacement current is taken into account in the total current.

In summary, we have shown how to describe ion transport in homogeneous channels at the mesoscopic level. The extension of the present considerations to the transport of several ionic species in one channel and to the case of heterogeneous channels of relevance to biological systems is possible on the basis of the present results.

Acknowledgments. D. A. is grateful to the F. R. S.-FNRS for financial support. This research is financially supported by the Belgian Federal Government (IAP project "NOSY") and the "Communauté française de Belgique" (contract "Actions de Recherche Concertées" No. 04/09-312).

Appendix A: Solution of the channel electrostatics

The electric potential Φ_i is defined on each cell $i = 1, ..., L$ and obeys the discretized Poisson equation (11) (above written in terms of the dimensionless potential $\phi = -e\Phi/k_{\rm B}T$). This linear system must be solved at each time the

particle distribution changes and must satisfy the boundary conditions

$$\Phi_0 = \Phi_{\rm L}, \quad \Phi_{L+1} = \Phi_{\rm R}\,. \tag{A1}$$

This linear system of equations can be written in matrix form as

$$\mathbf{C}\cdot\mathbf{\Phi} = \mathbf{Z} \tag{A2}$$

with the vectors

$$\mathbf{\Phi}^{\rm T} = (\Phi_1, ..., \Phi_L) \tag{A3}$$

and

$$\begin{aligned}\mathbf{Z}^{\rm T} &= e\,(N_1 - N_-, ..., N_L - N_-) + \alpha(\Phi_{\rm L}, 0, ..., 0, \Phi_{\rm R}) \\ &\equiv \mathbf{Q} + \alpha(\Phi_{\rm L}, 0, ..., 0, \Phi_{\rm R})\,,\end{aligned} \tag{A4}$$

where T denotes the transpose operation and where we introduced the charge vector $\mathbf{Q}$ of components $Q_k = e(N_k - N_-)$. Note that the boundary conditions appear on the first and last components of the vector $\mathbf{Z}$ multiplied by the quantity $\alpha = (\epsilon N_-)/(n_-\Delta x^2)$, which has the units of a capacitance. The $L\times L$ symmetric matrix $\mathbf{C}$ reads

$$\mathbf{C} = \alpha\begin{pmatrix} 2 & -1 & & & & \\ -1 & 2 & -1 & & & \\ & -1 & 2 & \ddots & & \\ & & -1 & \ddots & -1 & \\ & & & \ddots & 2 & -1 \\ & & & & -1 & 2 \end{pmatrix} \tag{A5}$$

It is invertible so that we have

$$\mathbf{\Phi} = \mathbf{C}^{-1}\cdot\mathbf{Z} \tag{A6}$$

with

$$\left(\mathbf{C}^{-1}\right)_{ij} = \begin{cases} \frac{i}{\alpha(L+1)}(L+1-j) & \text{if} \quad i \le j \\ \frac{j}{\alpha(L+1)}(L+1-i) & \text{if} \quad i > j\,. \end{cases} \tag{A7}$$

The matrix $\mathbf{C}^{-1}$ is symmetric, as it should.

The electrostatic energy U stored in the system is given by

$$U = \frac{1}{2}\mathbf{\Phi}^{\rm T}\cdot\mathbf{C}\cdot\mathbf{\Phi} = \frac{1}{2}\mathbf{Z}^{\rm T}\cdot\mathbf{C}^{-1}\cdot\mathbf{Z}\,. \tag{A8}$$

The change in electrostatic energy associated with the transition of an ion from cell i to cell $i+1$ is thus given by

$$\Delta U_{i,i+1} = \frac{1}{2}\left(\mathbf{Z'}^{\rm T}\cdot\mathbf{C}^{-1}\cdot\mathbf{Z'} - \mathbf{Z}^{\rm T}\cdot\mathbf{C}^{-1}\cdot\mathbf{Z}\right) \tag{A9}$$

where $Z'_k = Z_k - e\delta_{k,i} + e\delta_{k,i+1}$ characterize the change in the charge distribution resulting from the transition $i \to i+1$. Developing this expression yields

$$\Delta U_{i,i+1} = e(\Phi_{i+1} - \Phi_i) + \frac{e^2}{2}\left[\left(\mathbf{C}^{-1}\right)_{i,i} - 2\left(\mathbf{C}^{-1}\right)_{i,i+1} + \left(\mathbf{C}^{-1}\right)_{i+1,i+1}\right], \tag{A10}$$

where we used the symmetry of the coefficients $\left(\mathbf{C}^{-1}\right)_{i,j} = \left(\mathbf{C}^{-1}\right)_{j,i}$ as well as the expression $\Phi_j = \sum_k \left(\mathbf{C}^{-1}\right)_{j,k} Z_k$ for the electric potential in cell j. We see that the change in electrostatic energy $\Delta U_{i,i+1}$ only depends on the initial voltage difference plus a term independent of the charge state of the system. In the case where the transition involves

one of the reservoirs, say the left one, we have $\Phi'_{\rm L} = \Phi_{\rm L}$ and the change in electrostatic energy for a transition from the left reservoir to cell 1 reads

$$\Delta U_{0,1} = e(\Phi_1 - \Phi_{\rm L}) + \frac{e^2}{2}\left(\mathsf{C}^{-1}\right)_{1,1} \tag{A11}$$

and similarly for transitions involving the right reservoir. By virtue of expression (A6), we see that

$$\Phi'_j = \sum_k \left(\mathsf{C}^{-1}\right)_{j,k} Z'_k = \sum_k \left(\mathsf{C}^{-1}\right)_{j,k} (Z_k - e\delta_{k,i} + e\delta_{k,i+1}) = \Phi_j - e\left(\mathsf{C}^{-1}\right)_{j,i} + e\left(\mathsf{C}^{-1}\right)_{j,i+1}\,, \tag{A12}$$

which is Eq. (19) for the transition $i \to i+1$. Accordingly, the energy differences (A10) and (A11) can be expressed in terms of the initial and final voltage differences V_i and V'_i between the cells i and $i+1$ so that we recover Eq. (16) for the electrostatic energy difference. Note that Eq. (16) also holds for inhomogeneous channels with $\epsilon = \epsilon(x)$ and $n_- = n_-(x)$.

Appendix B: Macroscopic affinities of the stochastic model

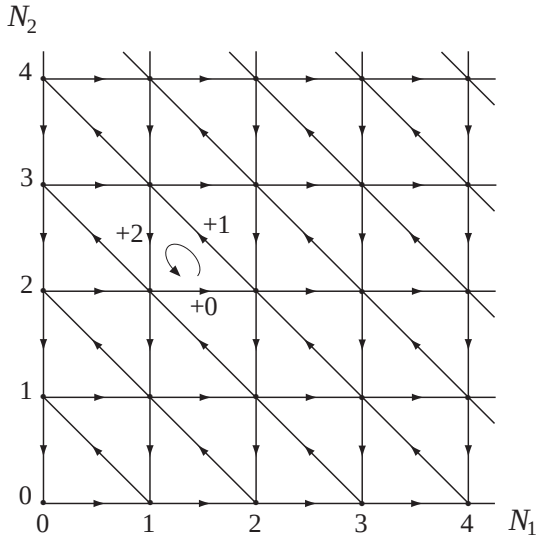

FIG. 5: Graph associated with the random process of the master equation (12) over a chain of length $L = 2$. The depicted cycle corresponds to the transfer of an ion from the left to the right reservoir. The orientations of the edges are chosen so that a movement from left to right is counted positively.

In this appendix, we detail the thermodynamic properties of the stochastic model introduced in Sec. III. For a system ruled by the master equation (12), a graph G is associated as follows [22]: each state ω of the system corresponds to a vertex or node while the edges represent the different transitions $\omega \rightleftharpoons \omega'$ allowed between the states. The stochastic ion transport of Sec. III is defined in terms of the populations $(N_1, ..., N_L)$ of mobile ions inside the channel. Accordingly, each such configuration defines a node of the graph and each transition $\pm i$ corresponds to one edge. As an example the graph associated with the case $L = 2$ is drawn in Fig. 5.

As a matter of fact, cyclic trajectories play a special role as they link the macroscopic thermodynamic properties to the transition rates of the mesoscopic description [22, 24]. In the case $L = 2$ corresponding to Fig. 5, we see that any cyclic path in the graph can be decomposed as a linear combination of two types of cyclic trajectories:

$$c_1 \equiv (N_1, N_2) \to (N_1+1, N_2) \to (N_1+1, N_2+1) \to (N_1, N_2+1) \to (N_1, N_2) \tag{B1}$$

and

$$c_2 \equiv (N_1, N_2) \to (N_1+1, N_2) \to (N_1, N_2+1) \to (N_1, N_2)\,. \tag{B2}$$

As shown by Schnakenberg [22], the macroscopic affinities associated with these cyclic paths can be obtained from the transition rates by calculating the quantities

$$A(c_1) = \ln \frac{W_{+0}(N_1,N_2)W_{-2}(N_1+1,N_2)W_{-0}(N_1+1,N_2+1)W_{+2}(N_1,N_2+1)}{W_{-0}(N_1+1,N_2)W_{+2}(N_1+1,N_2+1)W_{+0}(N_1,N_2+1)W_{-2}(N_1,N_2)} \tag{B3}$$

and

$$A(c_2) = \ln \frac{W_{+0}(N_1,N_2)W_{+1}(N_1+1,N_2)W_{+2}(N_1,N_2+1)}{W_{-0}(N_1+1,N_2)W_{-1}(N_1,N_2+1)W_{-2}(N_1,N_2)} \,. \tag{B4}$$

These expressions are obtained as the ratio between the product of the transition rates along the cyclic path in one direction over the product of the transition rates along the cyclic path in the reversed direction. Calculating the affinities (B3) and (B4) with the transition rates (14) yields

$$A(c_1) = 0 \quad \text{and} \quad A(c_2) = \ln\left(\frac{N_0}{N_{L+1}}\mathrm{e}^{\Delta\phi}\right) . \tag{B5}$$

The first one always vanishes whereas the second is the macroscopic affinity (21), irrespectively of the initial configuration $(N_1, ..., N_L)$. Note that $A(c_2)$ only involves externally controlled parameters, as it should. This results from the fact that only the second cycle involves the transport of an ion across the channel. The extension to larger channels, $L > 2$, is straightforward.

According to a result of Kolmogorov [57], a Markov process is at equilibrium if and only if the affinities along the cycles vanish. As shown by Eqs. (B5) this occurs when condition (9) is fulfilled.

[1] W.H. Nernst, Z. Phys. Chem. **2**, 613 (1888).
[2] W.H. Nernst, Z. Phys. Chem. **4**, 129 (1889).
[3] M. Planck, Ann. Physik und Chemie **39**, 161 (1890).
[4] M. Planck, Ann. Physik und Chemie, **40**, 561 (1890).
[5] M. Gouy, J. Physique **9**, 457 (1910).
[6] D. L. Chapman, Phil. Mag. **25**, 475 (1913).
[7] J. O'M. Bockris and A. K. N. Reddy, *Modern Electrochemistry* (New York, Plenum Press, 1970).
[8] B. Eisenberg, in *The Biophysics Textbook On Line: Channels, Receptors, and Transporters*, L. J. DeFelice, ed., (2000).
[9] J. D. Jackson, *Classical Electrodynamics* (Wiley and Sons, New York, 1999).
[10] H. Cohen and J. W. Cooley, Biophys. J. **5**, 145 (1965).
[11] Y. M. Blanter and M. Büttiker, Phys. Rep. **336**, 1 (2000).
[12] W. Shockley, Bell Syst. Techn. J. **28**, 33 (1949).
[13] I. Rubinstein, *Electro-Diffusion of Ions* (SIAM Studies in Applied Mathematics, SIAM, Philadelphia, PA, 1990)
[14] B. Alberts, D. Bray, A. Johnson, J. Lewis, M. Raff, K. Roberts, and P. Walter, *Essential Cell Biology* (Garland Publishing, New York, 1998).
[15] B. Hille, *Ionic Channels of Excitables Membranes* (Sinauer, Massachusetts, 2001).
[16] R. M. M. Smeets, U. F. Keyser, N. H. Dekker, and C. Dekker, Proc. Natl. Acad. Sci. U.S.A. **105**, 417 (2008).
[17] W. Nonner and B. Eisenberg, Biophys. J. **75**, 1287 (1998).
[18] P. Ramirez, V. Gomez, J. Cervera, B. Schiedt, and S. Mafe, J. Chem. Phys. **126**, 194703 (2007).
[19] D. Constantin and Z. S. Siwy, Phys. Rev. E **76**, 041202 (2007).
[20] E. Barsoukov and J.R. Macdonald, *Impedance spectroscopy: Theory, experiment, and applications* (Wiley-Interscience, 2005).
[21] G. Nicolis and I. Prigogine, Proc. Natl. Acad. Sci. USA **68**, 2102 (1971).
[22] J. Schnakenberg, Rev. Mod. Phys **48**, 571 (1976).
[23] G. Nicolis and I. Prigogine, *Self-Organization in Nonequilibrium Systems* (Wiley, New York, 1977).
[24] T. L. Hill, *Free Energy Transduction and Biochemical Cycle Kinetics* (Dover, New-York, 2005).
[25] E. Abad and J. J. Kozak, Physica A **380**, 172 (2007).
[26] E. Barkai, R. S. Eisenberg, and Z. Schuss, Phys. Rev. E **54**, 1161 (1996).
[27] P. Turq, F. Lantelme, and H. L. Friedman, J. Chem. Phys. **66**, 3039 (1977).
[28] S. Kuyucak, O. S. Andersen and S.-H. Chung, Rep. Prog. Phys. **64**, 1427 (2001).
[29] D. J. Evans, E. G. D. Cohen, and G. P. Morriss, Phys. Rev. Lett. **71**, 2401 (1993).
[30] G. Gallavotti and E. G. D. Cohen, Phys. Rev. Lett. **74**, 2694 (1995).
[31] J. L. Lebowitz and H. Spohn, J. Stat. Phys. **95**, 333 (1999).
[32] C. Maes, J. Stat. Phys. **95**, 367 (1999).
[33] U. Seifert, Phys. Rev. Lett. **95**, 040602 (2005).

[34] D. Andrieux and P. Gaspard, J. Stat. Phys. **127**, 107 (2007).
[35] R. J. Harris and G. M. Schütz, J. Stat. Mech.: Th. Exp. P07020 (2007).
[36] E. M. Sevick, R. Prabhakar, S. R. Williams, and D. J. Searles, Annu. Rev. Phys. Chem. **59**, 603 (2008).
[37] T. Teorell, Progr. Biophysics and Biophysic. Chem. **3**, 305 (1953).
[38] P. Debye and E. Hückel, Phys. Z. **24**, 185 (1923).
[39] C. W. Gardiner, *Handbook of Stochastic Methods for Physics, Chemistry and the Natural Sciences* (Springer-Verlag, 1990).
[40] L. Onsager, Phys. Rev. **37**, 405 (1931).
[41] R. C. Tolman, *The Principles of Statistical Mechanics* (Oxford University Press, Oxford, 1938).
[42] Several functions $\psi(\Delta U)$ can be chosen which satisfy the condition (20). Besides the function (15) which has been considered in another context [58], alternative functions are the Metropolis one $\psi(\Delta U) = (D/\Delta x^2)\min\left\{1, \mathrm{e}^{-\beta\Delta U}\right\}$, or the Kawasaki one $\psi(\Delta U) = (D/\Delta x^2)[2/\left(1+\mathrm{e}^{\beta\Delta U}\right)]$, which also satisfy the condition (20) [59]. The specific form of the function $\psi(\Delta U)$ should be determined by the microscopic process ruling the jumps of particles between the cells. We emphasize that, in our case, the energy difference ΔU depends on the global configuration because of the long-range Coulomb interaction. This dependence is required in order to obtain a model which is thermodynamically consistent, irrespectively of the specific choice of the function ψ.
[43] T. De Donder and P. Van Rysselberghe, *Thermodynamic Theory of Affinity* (Stanford University Press, Menlo Park, 1936).
[44] D. T. Gillespie, J. Comp. Phys. **22**, 403 (1976).
[45] S. Ramo, Proc. IRE. **27**, 584 (1939).
[46] W. Shockley, J. Appl. Phys. **9**, 635 (1938).
[47] W. Nonner, A. Peyser, D. Gillespie, and B. Eisenberg, Biophys. J. **87**, 3716 (2004).
[48] P. Gaspard and X.-J. Wang, Phys. Rep. **235**, 291 (1993).
[49] W. Schottky, Ann. Phys. **57**, 541 (1918).
[50] D. Andrieux and P. Gaspard, J. Stat. Mech.: Th. Exp. P02006 (2007).
[51] D. Andrieux and P. Gaspard, J. Stat. Mech.: Th. Exp. P01011 (2006).
[52] B. Cleuren, C. Van den Broeck, and R. Kawai, Phys. Rev. E **74**, 021117 (2006).
[53] B. Derrida, J. Stat. Mech.: Th. Exp. P07023 (2007).
[54] A. M. Berezhkovskii and S. M. Bezrukov, Phys. Rev. Lett. **100**, 038104 (2008).
[55] A. M. Berezhkovskii and S. M. Bezrukov, J. Phys. Chem. B **112**, 6228 (2008).
[56] D. Andrieux and P. Gaspard, J. Stat. Mech.: Th. Exp. P11007 (2008).
[57] A. N. Kolmogorov, Math. Ann., **112**, 155 (1936).
[58] H. Wang, C. S. Peskin, and T. C. Elston, J. Theor. Biol. **221**, 491 (2003).
[59] H. Spohn, *Large Scale Dynamics of Interacting Particles* (Springer, Heidelberg, 1991).